

Fig. 6. A family of polygon cross sections suited for the same rule as the preceding figures.

rically equal triangles not arranged on a half side but on a whole side of the inner regular octagon. Furthermore, two geometrically equal triangles are not right-angled. The exact wave resistance becomes (because $R_{\square}=1$)

$$R = R_0/8$$

and $r_2=1.765$ and $r_4=4.262$.

Fig. 6(b), having five geometrically equal right-angled triangles, is symmetrical with three mirror lines, though the inner regular hexagon has six mirror lines. The exact wave resistance is

$$R = \frac{1}{6} \frac{K'(k)}{K(k)} R_0 = 0.09298 R_0$$

where

$$k = \sqrt{\frac{2(\cos \pi/5 - \cos 3\pi/5)}{(1 - \cos 3\pi/5)(1 + \cos \pi/5)}} = 0.9713.$$

The radii are $r_2=1.5$ and $r_4=2.0$.

In Fig. 6(c), two geometrically equal triangles are not right-angled, and they are arranged on a whole side of the outer regular octagon. This case can be considered to be the inversion of Fig. 6(a). Therefore, the exact wave resistance is the same as Fig. 6(a). The radii are $r_2=1.631$, $r_3=0.4142$, and $r_4=1.765$.

In Fig. 6(d), both of the inner and outer conductors are not equiangular polygons. This case is considered as a slight variation for $n=3$ of Fig. 2 having three geometrically equal right-angled triangles. The wave resistance is equal to Fig. 2 because the procedure of mapping to a semi-circle is similar to Fig. 2. Fig. 6(d) has $R=0.1303R_0$, $r_2=1.609$, $r_3=0.5877$, and $r_4=2.433$.

V. CONCLUSION

Some shapes of coaxial inner and outer regular polygonal conductors can be exactly evaluated on their wave resistance.

The following special cases of this paper coincide with Wheeler [1]:

	Herein	Wheeler
Fig. 1	$n=2$	Fig. 23
	$n=3$	25
	$n=4$	25
Fig. 2	$n=2$	26
	$n=4$	26
Fig. 3	$n=2$	26.

REFERENCES

- [1] H. A. Wheeler, "Transmission-line conductors of various cross sections," *IEEE Trans. Microwave Theory Tech.*, vol. MTT-28, pp. 73-83, Feb. 1980.
- [2] H. J. Riblet, "An accurate determination of the characteristic impedance of the coaxial system consisting of a square concentric with a circle," *IEEE Trans. Microwave Theory Tech.*, vol. MTT-23, pp. 714-715, Aug. 1975.
- [3] H. J. Riblet, "An expansion of the Terakado solution with an application," *IEEE Trans. Microwave Theory Tech.*, vol. MTT-30, pp. 2036-2039, Nov. 1982.
- [4] R. Terakado, "The characteristic impedance of rectangular coaxial line with ratio 2:1 of outer-to-inner conductor side length," *IEEE Trans. Microwave Theory Tech.*, vol. MTT-24, pp. 124-125, Feb. 1976.

Analysis of the Transmission Characteristics of Inhomogeneous Grounded Finlines

ADALBERT BEYER

Abstract—This paper describes a concept for an efficient design of finline tapers that is especially useful in cases when certain quantities have been prescribed with respect to reflection loss and bandwidth. Since abrupt discontinuities are neglected, the analysis is applicable to smooth finline tapers only.

Various contour functions are investigated for the taper optimization. Experimental results for optimized tapers confirm the design theory.

I. INTRODUCTION

Smooth inhomogeneous finlines have already been used as broad-band components like transformers, attenuators, detectors, mixers, and nonreciprocal elements [1], [2], [5].

In the beginning, the design of inhomogeneous finlines was mainly done experimentally, i.e., the cross sections of these tapers had been designed with a general parabolical dependence of the slot widths ($2s$) on the length coordinate (z) with the exponent of the parabola having been determined experimentally [5].

Recently, there have been publications of nonexperimental design procedures, e.g., in [6], where the use of a spectral-domain approach has been suggested. Another concept [9], which considers inhomogeneous finlines that consist of an infinite number of elementary homogeneous finline sections, has proved the realizability of this line.

This paper follows the method presented in [4], which has the considerable advantage of taking into account the influence of the thickness of the metallization and of the longitudinal slits in the housing.

Manuscript received May 2, 1984; revised September 4, 1984.

The author is with Fachgebiet Allgemeine und Theoretische Elektrotechnik, Department of Electrical Engineering, Duisburg University, Bismarckstrasse 81, D-4100 Duisburg 1, Federal Republic of Germany.

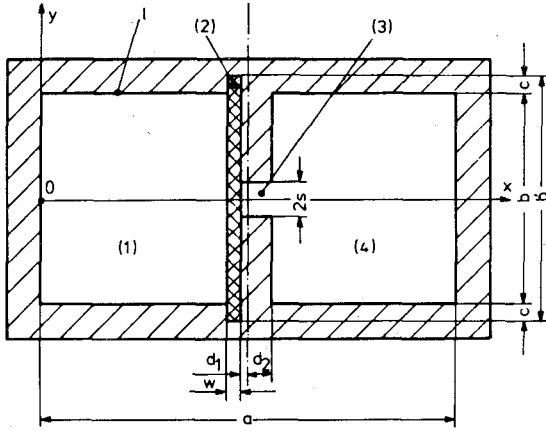


Fig. 1. Geometry of the unilateral grounded finline section.

II. THE METHOD

Consider the cross section of a finline placed on the lossless conductor and having a closed boundary l (Fig. 1).

All the electromagnetic fields inside the waveguide are expressible in terms of the Hertz potentials Φ and Ψ . The z dependence of the fields can be described employing a linear combination of $\exp(\gamma z)$ and $\exp(-\gamma z)$, where γ is the propagation factor. The time dependence of the electromagnetic fields $\exp(j\omega t)$ is omitted in the following train of thought.

If the problem of the inhomogeneous finline is to be solved, it is a fundamental supposition that the properties of the homogeneous finline above are known accurately, considering even second-order effects like the metallization thickness d and the supporting slit in the waveguide mount c . Thus, a complete study of the grounded unilateral finline is given by [3], where the eigenvalue equation system is solved by applying the Ritz-Galerkin method. Using the results of this method, the eigenvalues p_{mn} , the electromagnetic fields, the effective dielectric constants $\epsilon_{\text{eff}, mn}$, as well as the characteristic impedance Z_{0mn} of finlines can be calculated as a function of the geometrical dimensions and the above-mentioned second-order effects.

Next, consider the longitudinal section of a finline (3) shown in Fig. 2 which is terminated by homogeneous finlines (1) and (2) on the left- and on the right-hand side.

The transmission and the reflection properties of the problem mentioned above can be calculated by using the generalized telegraphists's equations for waveguides of varying cross section [8]

$$-\frac{\partial U_m}{\partial z} = \gamma_m Z_m I_m - \sum_{n=0}^{\infty} C_{nm} U_n \quad (1)$$

$$-\frac{\partial I_m}{\partial z} = \frac{\gamma_m}{Z_m} U_m + \sum_{n=0}^{\infty} C_{mn} I_n \quad (2)$$

where $U_m(z)$ and $I_m(z)$ are the m th modal voltage and current of the considered inhomogeneous finline, respectively; Z_m is the m th modal characteristic impedance of the above line. The coupling coefficient C_{mn} between the m th and n th modal is given by

$$C_{mn} = \int_A \vec{e}_n \cdot \frac{\partial \vec{e}_m}{\partial z} dA \quad (3)$$

where \vec{e}_n and \vec{e}_m are the n th and m th orthogonal vector functions, respectively. The surface integral is extended over A the total cross section of the inhomogeneous finline. In (2), the influence of the dielectric constant $\epsilon_{\text{eff}, m}$ on the slot width $2s(z)$

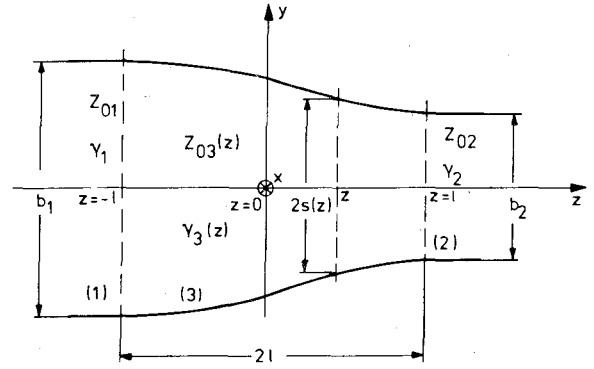


Fig. 2. Longitudinal section of an inhomogeneous finline.

must be taken into account via

$$\frac{\gamma_m}{jZ_m} = j\omega\epsilon_0\epsilon_{\text{eff}, m}(z) + \frac{p_{m,1}^2}{j\omega\mu_0} \quad (4)$$

where p_m is the m th eigenvalue of the inhomogeneous finline.

In the case of the quasi-TE₁₀-mode propagation in the inhomogeneous finline, substitution of the voltage reflection factor Γ in the general equations (1) and (2) leads to the following expression:

$$\frac{d\Gamma_3(z)}{dz} - 2\gamma_3(z)\Gamma_3(z) + (1 - \Gamma_3^2(z)) \left(\frac{1}{2} \frac{d \ln K_3(z)}{dz} - C_{11} \right) = 0 \quad (5)$$

which is a Riccati's differential equation.

In order to solve this differential equation, look at the contour function given by

$$f(z) = \begin{cases} 0, & -\infty \leq z < -l \\ \frac{1}{2} \frac{d \ln K_3(z)}{dz}, & -l < z < +l \\ 0, & +l < z \leq \infty \end{cases} \quad (6)$$

The value $K_3(z)$ is defined as

$$K_3(z) = \frac{\sqrt{\frac{\mu_0}{\epsilon_0}}}{\sqrt{\epsilon_{\text{eff}} - \left(\frac{\lambda_0}{\lambda_c}\right)^2}} \quad (7)$$

where ϵ_{eff} and λ_c are the effective dielectric constant and λ_c the cutoff wavelength of the quasi-TE₁₀-mode propagation on the inhomogeneous finline section, respectively. The known incident wave is excited at $z = -\infty$ and the waveguide is properly terminated at $z = +\infty$.

The characteristic impedance Z_0 of a lossless waveguide is a real function; consequently, its contour function $f(z)$ must also be real

$$f(z) = f^*(z). \quad (8)$$

Thus, in order to examine the realizability of the given contour function $f(z)$, the following quadratic integral must exist (Paley-Wiener's theorem):

$$\int_{z=-\infty}^{z=+\infty} |f(z)|^2 dz. \quad (9)$$

As the Riccati's differential equation (5) will be solved numerically, for this purpose the impedance function $K_3(z)$ is expanded

into a series given by

$$K_3(z) = \begin{cases} 0, & -\infty \leq z < -l \\ \sum_{n=0}^P a_n z^n, & -l < z < +l \\ 0, & l < z \leq +\infty \end{cases} \quad (10)$$

By introducing this series expansion into the formula for the contour function $f(z)$ ((6)) and by using a well-known series expansion of the logarithmic function, the following form of the contour function can be found:

$$f(z) = \begin{cases} 0, & -\infty \leq z < -l \\ \frac{1}{2} \sum_{p=0}^{Q(P-1)} (p+1) \left(\sum_{q=1}^Q \frac{(-1)^{q+1}}{q} a_{p+1}^q \right) z^p, & -l < z < +l \\ 0, & +l < z \leq +\infty. \end{cases} \quad (11)$$

In this equation, a_{p+1} is a coefficient which is closely connected to the expansion coefficients a_n of the impedance function $K_3(z)$. Now, if the propagation factor $\gamma_3(z)$ is also expanded into a series given by

$$\gamma_3(z) = \sum_{m=0}^P b_m z^m \quad (12)$$

and if the function $g(z)$, which is defined as

$$g(z) = f(z) - C_{11}^{(3)} = \sum_{k=0}^P g_k z^k \quad (13)$$

is substituted for the function $f(z)$ shown above ((11)), the Riccati's differential equation can easily be solved if the reflection coefficient r_3 is also formulated as

$$\Gamma_3(z) = \sum_{r=0}^{\infty} \Gamma_r ((z - z_0) k_T)^r. \quad (14)$$

By using the known condition for the reflection coefficient

$$\Gamma_3(z=l) = 0 \quad (15)$$

it can be shown that the expansion coefficient Γ_0 of the series for $\Gamma_3(z)$ in (14) is zero. The value k_T of the introduced coordinate transformation is used to optimize the convergence behavior of this numerical solution. Thus, the reflection coefficient $\Gamma_3(z)$ can be found as a function of the frequency and of the expansion coefficients of the impedance function $K_3(z)$. Two kinds of solutions of the Riccati's differential equation are possible.

1) If the impedance function $K_3(z)$ is known at P different coordinate values z_n for a given frequency $f = f_0$, the Riccati's differential equation can be solved for the unknown reflection coefficients by finding the zeros of the above-mentioned differential equation numerically.

2) If a function $\Gamma_3(z)$, i.e., the reflection coefficient is given as a function of the frequency f at the P frequency points, $(P+1)$ equations can be derived for the $(P+1)$ unknown coefficients a_n of the series expansion of $K_3(z)$. In this case, it must be made sure that the contour function $f(z)$ is realizable (see (6) and (9)).

III. NUMERICAL AND EXPERIMENTAL RESULTS

During the numerical investigations, five different shapes of inhomogeneous finlines have been analyzed: the exponential taper, the near-optimum taper [4], the linear taper, the taper of the second-order degree, and the taper of the fourth-order degree.

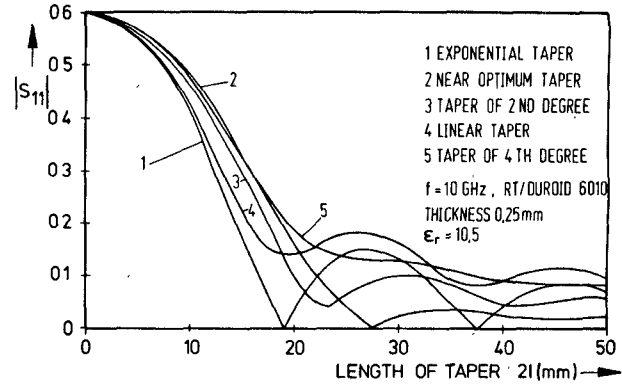


Fig. 3. The eigenreflection coefficient of the investigated tapers.

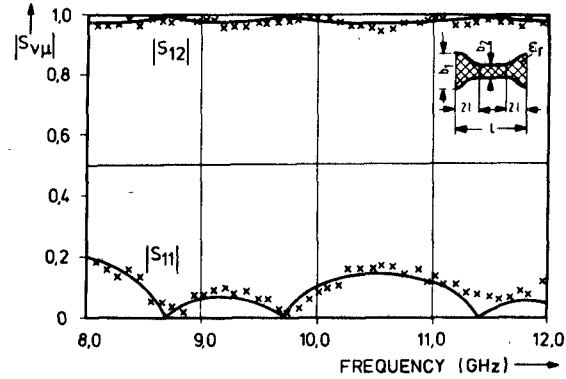


Fig. 4. The calculated and measured scattering parameters of a two-taper section as a function of the frequency.

The eigenreflection coefficient of the input port of these tapers is shown in Fig. 3 as a function of the length $2l$ for tapers on a RT/Duroid 6010 substrate material at 10 GHz.

These types of tapers lead to a realizable contour function; this means that besides being real this function is well defined in the interval of the inhomogeneous finline for z -values between $-l$ and $+l$ and that it is quadratically integrable. By means of the developed theory and an optimization procedure, the length of the taper can be minimized for given reflection coefficients by changing the coefficients a_n of the series in (10), which describe the contour function indirectly.

Fig. 4 serves as an example; it shows the calculated and measured scattering parameters of a two-taper section; geometrically, the slot has the character of an exponential function.

By using the theoretical results for inhomogeneous finlines, a broad-band pin diode attenuator has been developed for an X-band system to measure the magnetic and the dielectric material parameters. This attenuator employs a similar two-taper section as given by Fig. 4. The designed two-taper section must have less than a 0.3-dB transmission loss and a reflection loss higher than 22 dB. Here, a near-optimum taper with less than a 0.1-dB transmission loss and a reflection loss higher than 30 dB has been chosen as an inhomogeneous finline section. With these requirements, the near-optimum transformers are designed on an isotropic substrate with a thickness of 0.125 mm and a dielectric constant $\epsilon_r = 2.22$ (RT/Duroid 5880). The optimum design of

TABLE I

s_0	.2199527160E+00
s_1	6009339206E-02
s_2	-1497378521E+00
s_3	3037782331E+01
s_4	1154783127E+02
s_5	-8920013427E+01
s_6	7731410547E+01
s_7	-4859313889E+01
s_8	1854203359E+01
s_9	3181239616E+00

the contour function is obtained, if the input reflection coefficient $s_{11} = \Gamma_3(z = -l)$ for the full X-band ($f_1 = 8$ GHz, $f_2 = 12.5$ GHz) is kept below a prescribed limit of 0.1 dB. In this case, an optimum length of taper of $2l = 50$ mm has been found. The slot width of the taper section is determined by

$$y = s(z) = \sum_{n=0}^9 \frac{s_n}{2} \left(\frac{l-z}{2l} \right)^n, \quad -l < z < +l. \quad (16)$$

Table I shows the coefficients of this power series s_n for this design.

The geometrical dimensions, as well as the transmission properties of the optimized two-taper section, are shown in Fig. 5.

Although this device has a transmission loss of < 0.2 dB, the reflection loss of 22 dB is smaller than the 26 dB calculated by the above theory. This is a consequence of the fact that the dielectric loss and the discontinuities between the rectangular waveguide and the inhomogeneous finline section in the theory have been neglected. The dielectric loss is about 0.1–0.12 dB over the total X-band. Since the copper sheet on the substrate rusts rapidly, the copper must be coated with a thin gold sheet for the application as a pin diode attenuator. It has to be noted that the quality of the transmission properties is decreased in this case (see Fig. 5).

Next, the method described above will be explained by using an impedance exponential taper as an example. As follows from the Paley–Wiener approximation theory, the contour function of the impedance exponential taper is also a realizable function, i.e., the quadratic integral given by (9) is bounded. The required two-taper section is designed to have a return loss higher than 26 dB over the total Ka-band. Fig. 6 shows the transmission and reflection coefficients for a two-taper section consisting of two identical impedance exponential tapers. This finline structure can be used as an antenna in finline technique.

In all of these cases, the convergence has been good and the computing time has been relatively short (approximately 0.03 s for one frequency point on a Control Data CYBER 76 computer). The measurements have been made using an automatic network analyzer.

IV. CONCLUSIONS

A simple modification of an existing design technique for rectangular waveguide transitions has been employed to obtain a plain and fast description of tapers in finline technique. For practical applications, several tapers have been designed using

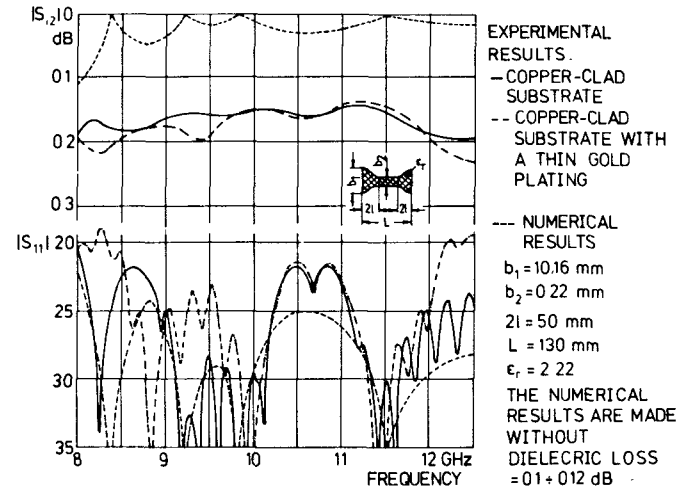


Fig. 5. The calculated and the measured values of the reflection coefficient $|s_{11}|$ and the transmission coefficient $|s_{21}|$ of a symmetrical two-taper section.

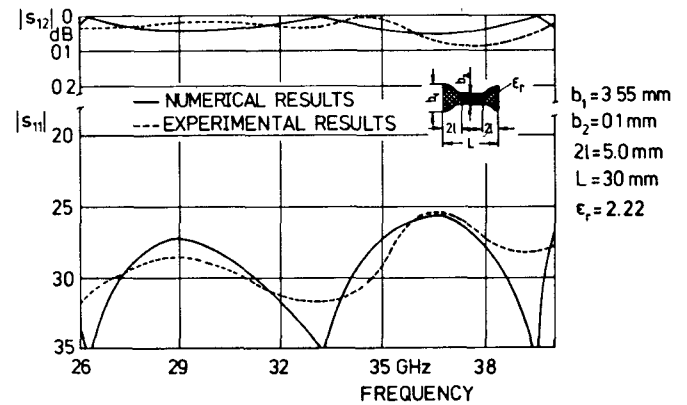


Fig. 6. The transmission and the reflection coefficient of a symmetrical two-taper section (the thickness of the RT/Duroid substrate is equal 0.125 mm).

this technique, and they have successfully been tested for the X- and the Ka-band.

The required inhomogeneous finline structures for some integrated millimeter-wave devices, like attenuators, oscillators, isolators, circulators, etc., have already been realized by employing this method.

REFERENCES

- [1] R. N. Bates and M. D. Coleman, "Millimeter-wave finline balanced mixers," in 1979 IEEE MTT-S Int. Microwave Symp. Dig., (Orlando), pp. 721–725.
- [2] G. Begemann, "An X-band balanced fin-line mixer," *IEEE Trans. Microwave Theory Tech.*, vol. MTT-26, pp. 1007–1011, Dec. 1978.
- [3] A. Beyer and I. Wolff, "A solution of the earthed fin line with finite metallization thickness," in 1980 IEEE MTT-S Int. Microwave Symp. Dig., (Washington, DC), pp. 258–260.
- [4] A. Beyer and I. Wolff, "Calculation of the transmission properties of inhomogeneous fin lines," in *Proc. 10th Eur. Microwave Conf.*, (Warsaw, Poland), 1980, pp. 322–326.
- [5] H. Hofmann, H. Meinel, and B. Adelseck, "New integrated mm-wave components using fin-lines," in 1978 IEEE MTT-S Int. Microwave Symp. Dig., (Ottawa, Canada), pp. 21–23.
- [6] D. Mirshekar-Syahkal and J. B. Davies, "Accurate analysis of tapered planar transmission lines for microwave integrated circuits," *IEEE Trans. Microwave Theory Tech.*, vol. MTT-29, pp. 123–128, Feb. 1981.
- [7] J. R. Pyle and R. J. Angle, "Cutoff wavelengths of waveguides of unusual cross sections," *IEEE Trans. Microwave Theory Tech.*, vol. MTT-12, pp. 556–557, Sept. 1964.
- [8] G. Reiter, "Generalized telegraphist's equations for waveguides of varying cross-section," *Proc. Inst. Elec. Eng.*, (B) 106, pp. 54–57, 1959.

- [9] A. M. K. Saad and Schünemann, "Design of fin-line tapers, transitions, and couplers," in *Proc. 11th Eur. Microwave Conf.*, (Amsterdam, The Netherlands), 1981, pp. 305-308.
- [10] L. Solymar, "Spurious modes in nonuniform waveguides," *IRE Trans. Microwave Theory Tech.*, vol. MTT-7, pp. 379-383, July 1959.
- [11] Ch. P. Womack, "The use of exponential transmission lines in microwave components," *IRE Trans. Microwave Theory Tech.*, vol. MTT-10, pp. 124-132, Mar. 1962.

Phase-Matched Waveguide Using the Artificial Anisotropic Structure and its Application to a Mode Converter

TETSUYA MIZUMOTO, STUDENT MEMBER, IEEE, HIROHIKO YAMAZAKI, AND YOSHIYUKI NAITO, SENIOR MEMBER, IEEE

Abstract—Phase matching by the artificial anisotropic structure and its application to a mode converter are proposed for millimeter-wave dielectric circuitry. A phase-matched dielectric planar waveguide is designed and mode conversion characteristics are studied. An experimental result of the nonreciprocal mode converter are presented to show the usefulness of the structure.

I. INTRODUCTION

As a transmission medium for low-cost integrated circuitry, dielectric waveguides have been studied in the millimeter-wave frequency range. Couplers and filters were designed in dielectric waveguide forms and realized with good performances [1], [2]. Nonreciprocal devices, such as isolators and circulators, were also studied [3]. As the waveguiding property of dielectric waveguides in millimeter-wave frequencies is very similar to that in optical frequencies, some devices in dielectric waveguide forms are interesting for optical integrated circuits.

There has been proposed an optical isolator making use of mode conversion between two cross-polarized modes [4], [5]. In order to obtain sufficient mode coupling in these devices, it is necessary to realize phase matching between the modes in question. This means that the propagation velocities in the waveguide must be equalized. This also gives rise to a great difficulty for realizing a practical device.

In this paper, as a simulation to optical applications, we propose a method for equalizing the propagation constants of the two cross-polarized modes in a dielectric waveguide. The proposed waveguide (Fig. 1) is called an artificial anisotropic waveguide. This technique can be applied with no difficulty to waveguide-type mode converters and/or isolators. A similar waveguide has been proposed and designed for optical applications [6]. The optical artificial anisotropic waveguide consists of dielectric thin film loaded by dielectric strips. In the proposed waveguide for millimeter-wave, dielectric strips are replaced by thin conductor strips, for a conductor can be regarded as a dielectric of infinite permittivity in this frequency range.

We first describe an analytical procedure to calculate the propagation velocity in the artificial anisotropic waveguide and show an example of a design of phase-matched waveguide. Mode conversion characteristics are also examined numerically for the

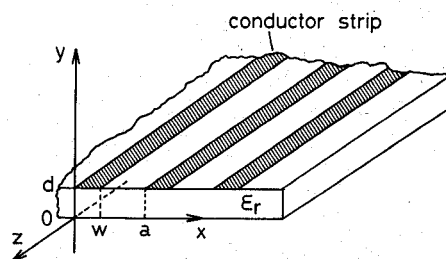


Fig. 1. The artificial anisotropic waveguide for millimeter-waves.

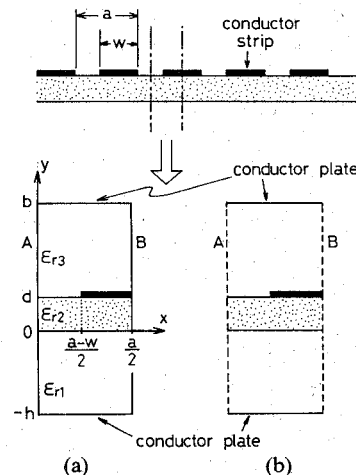


Fig. 2. Cross-sectional view of the artificial anisotropic waveguide and the structures to be analyzed. Both the planes A and B are electric walls in (a) and magnetic walls in (b).

waveguide containing magnetic anisotropy. Finally, the mode conversion observed in a fabricated waveguide is reported.

II. PHASE-MATCHING CONDITION AND MODE CONVERSION CHARACTERISTICS

Fig. 1 shows the proposed waveguide structure, which consists of a dielectric slab of thickness d loaded by conductor strips of width w . The structure extends infinitely in the x - z plane. The propagation direction is along the z axis. All the materials of the waveguide are assumed to be lossless. The dielectric has a relative dielectric constant ϵ_r .

Propagating electromagnetic fields are numerically analyzed by using a method similar to that described in [7]. For simplicity of analysis, the conductor strips loading the guiding layer are placed periodically in the x direction. The periodicity is not necessary for the operating principle. For the electromagnetic fields to satisfy the periodicity in the x direction, transverse boundary conditions are restricted to the two types as shown in Fig. 2. In Fig. 2 (a), both the planes A and B are electric walls and in (b) magnetic walls. The eigenmodes can be classified into two groups, corresponding to the boundary conditions of Fig. 2(a) or (b). The former determines E^x modes and the latter E^y modes. Hypothetical conductor plates are placed at $y = -h$ and b for convenience of analysis.

When the scalar potentials for TM and TE waves are defined by $\psi^{(e)}$ and $\psi^{(h)}$, respectively, the electromagnetic fields of hybrid modes, which actually propagate in the waveguide, are given by [7, eq. (1)].

After applying the boundary conditions on both the hypothetical conductor plates and the side walls, one obtains the scalar

Manuscript received June 14, 1984; revised September 4, 1984.

The authors are with the Department of Electrical and Electronic Engineering, Tokyo Institute of Technology, 2-12-1 Ookayama, Meguro-Ku, Tokyo, 152 Japan.